Letter

Supersolid phase in the diluted Holstein model

Jingyao Meng [1], Yuxi Zhang,[2] Rafael M. Fernandes [2], Tianxing Ma [1,3,*] and R. T. Scalettar [4]

[1]*School of Physics and Astronomy, Beijing Normal University, Beijing 100875, China*

[2]*School of Physics and Astronomy, University of Minnesota, Minneapolis, Minnesota 55455, USA*

[3]*Key Laboratory of Multiscale Spin Physics (Ministry of Education), Beijing Normal University, Beijing 100875, China*

[4]*Department of Physics and Astronomy, University of California, Davis, California 95616, USA*

(Received 8 July 2024; revised 12 November 2024; accepted 4 December 2024; published 24 December 2024)

The Holstein model on a square lattice at half-filling has a well-established finite temperature phase transition to an insulating state with long range charge density wave (CDW) order. Because this CDW formation suppresses pairing, a superconducting (SC) phase emerges only with doping. In this work, we study the effects of dilution of the local phonon degrees of freedom in the Holstein model while keeping the system at half filling. We find not only that the CDW remains present up to a dilution fraction $f \sim 0.15$, but also that long range pairing is stabilized with increasing f, resulting in a supersolid regime centered at $f \approx 0.10$, where long range diagonal and off-diagonal correlations coexist. Further dilution results in a purely SC phase, and ultimately in a normal metal. Our results provide a new route to the supersolid phase via the introduction of impurities at fixed positions which both increase quantum fluctuations and also are immune to the competing tendency to phase separation often observed in the doped case.

DOI: 10.1103/PhysRevB.110.L220506

Introduction. A regular arrangement of particle positions on the one hand, and particle mobility on the other, are typically competing tendencies. Nevertheless, the possibility of the coexistence of crystalline order and the most extreme type of transport, superfluid flow, was considered in Helium almost seven decades ago [1–4]. Although experimental confirmation in Helium was controversial [5–7], studies of several model Hamiltonians exhibiting such "supersolid" (SS) properties have been reported [8–13]. In electronic models, a supersolid phase is often identified by the coexistence between an insulating phase that breaks translational symmetry (such as a charge density wave, CDW) and a phase displaying off-diagonal long-range order (such as superconductivity, SC). Until now, supersolidity continues to be an intriguing area of quantum matter research, including novel solid state realizations such as "spin" supersolids like $Na_2BaCo(PO_4)_2$ [14] and $K_2Co(SeO_3)_2$ [15]. More broadly, continuous systems such as ultracold quantum gases offer the new platforms to achieve the realization of supersolidity [16–19], and this kind of supersolidity with continuous translational symmetry breaking is distinguished from the one in the lattice Hamiltonian with discrete translational symmetry.

The Holstein Hamiltonian [20], where the electronic site density is coupled to a local (dispersionless) oscillator mode, offers a possible arena in which to explore supersolid behavior. At half-filling, $\langle n \rangle = 1$, the low temperature phase exhibits CDW order and is insulating. The transition temperature $T_{\rm cdw}$ has been determined on a square lattice both via quantum Monte Carlo (QMC) simulations [21–23] and machine learning methods [24], thus firmly establishing the existence of a finite temperature transition to a commensurate solid.

One of the key properties of the Holstein Hamiltonian in the dilute limit is polaron formation, in which an electron localized to a site rearranges the local phonon configuration. As a result, when the electron moves, it must carry the lattice distortion along. Since Holstein polarons are quite heavy, as their density increases to the point where condensation into a superconducting phase becomes possible, the resulting critical temperatures are very low [25]. While a SC phase has been established [26–28], no coexistence of SC and CDW order has been observed in QMC studies of the Holstein model as the filling is varied [29–31], although a projector renormalization group method does report a supersolid at very weak coupling [32].

Supersolids are linked to the high mobility of quantum fluctuation vacancies in the otherwise ordered background of particle positions. A rather delicate balance is thus required: the doping must be light enough to allow the rigid pattern to coexist with the holes, yet sufficient quantum fluctuations are needed to form a condensate. Moreover, the tendency of the vacancies to phase separate from the ordered background must also be avoided. Here we demonstrate, using QMC simulations, a new route to supersolid behavior in an electron-phonon model in which the number of fermions remains commensurate (i.e., no doping is introduced), but the dilution is instead introduced in the bosonic degrees of freedom to which they couple. Through this way, it provides an interesting possibility to establish the physical system for supersolids both experimentally and theoretically. We show that measurements of the charge structure factor, superfluid susceptibility, compressibility, and spectral function form a consistent picture of the traversal of a CDW-SS-SC-normal

*Contact author: txma@bnu.edu.cn

sequence of phases as the dilution of the phonon modes increases. Our approach bears conceptual similarities to the investigations of supersolidity in Helium in that the dilution of phonon modes provides a random landscape analogous to the nanometer scale pore size of the Vycor glass in which the solid Helium is placed.

Model and method. The Holstein Hamiltonian [20],

$$\hat{\mathcal{H}} = -t \sum_{\langle \mathbf{i},\mathbf{j}\rangle,\sigma} (\hat{d}^{\dagger}_{\mathbf{i}\sigma}\hat{d}_{\mathbf{j}\sigma} + \text{H.c.}) - \mu \sum_{\mathbf{i},\sigma} \hat{n}_{\mathbf{i},\sigma} + \omega_0 \sum_{\mathbf{i}} \hat{a}^{\dagger}_{\mathbf{i}}\hat{a}_{\mathbf{i}} + \sum_{\mathbf{i},\sigma} g_{\mathbf{i}}\, \hat{n}_{\mathbf{i}\sigma}(\hat{a}^{\dagger}_{\mathbf{i}} + \hat{a}_{\mathbf{i}}), \tag{1}$$

describes electrons of spin $\sigma = \uparrow, \downarrow$ hopping between nearest-neighbor sites $\langle \mathbf{i}, \mathbf{j}\rangle$, and interacting with a local phonon mode on each site. In Eq. (1), $\hat{d}^{\dagger}_{\mathbf{i}\sigma}(\hat{d}_{\mathbf{i}\sigma})$ are fermion creation (destruction) operators with the given site and spin indices and with corresponding number operator $\hat{n}_{\mathbf{i}\sigma} = \hat{d}^{\dagger}_{\mathbf{i}\sigma}\hat{d}_{\mathbf{i}\sigma}$, whereas $\hat{a}^{\dagger}_{\mathbf{i}}(\hat{a}_{\mathbf{i}})$ are phonon creation (destruction) operators. The parameters t, ω_0 are the hopping energy (which we set to be our energy scale, $t = 1$) and phonon frequency, respectively, $g_{\mathbf{i}}$ is the electron-phonon coupling, and μ is the chemical potential. For the clean system with $g_{\mathbf{i}} = g$, the chemical potential corresponding to half-filling is $\mu_0 = -2g^2/\omega_0$.

We introduce dilution by allowing for a random, site-dependent, electron-phonon coupling $g_{\mathbf{i}}$, such that the coupling vanishes on a fraction f of the sites:

$$g_{\mathbf{i}} = \begin{cases} g & 1-f \\ 0 & f. \end{cases} \tag{2}$$

We consider $N = L \times L$ square lattices. Simulations are typically averaged over five to ten realizations of the random locations. If fN is not an integer, we calculate a weighted average of its adjacent integers, providing further disorder averaging. Further discussion is found in the Supplemental Material [33] (see also Refs. [34–46] therein).

We investigate the competition between SC and CDW order through the determinant quantum Monte Carlo (DQMC) method [31,47,48], an unbiased auxiliary-field approach for the computation of finite-temperature properties. We perform the usual mapping of the quantum oscillator degrees of freedom onto a path integral in imaginary time by discretizing the inverse temperature $\beta = \Delta\tau L_{\tau}$ [49], then the degrees of freedom of the fermions moving in this fluctuating space and imaginary time phonon field can be integrated out analytically. Since the fermionic operators appear quadratically in the Holstein Hamiltonian, they can be integrated out analytically. This results in an action that is the square of the determinant of a matrix and that depends on the space and imaginary-time dependent quantum phonon field, which is then sampled stochastically. The square in the determinant arises because the determinants of the up and down fermions are identical, i.e., there is no sign problem. The discretization mesh $\Delta\tau$ of the inverse temperature $\beta = 1/T$ was chosen small enough so that the "Trotter errors" are smaller than those associated with the statistical sampling. We set the system to half filling with charge density $\langle n\rangle = 1$, and define the dimensionless electron-phonon coupling $\lambda_D = g^2/(zt\omega_0)$, where $z = 4$ is the coordination number for the square lattice. In this work, we mainly focus on systems with $g = 1$, $\omega_0 = 1$ ($\lambda_D = 0.25$) and $g = 2$, $\omega_0 = 3$ ($\lambda_D = 0.33$), but also provide some results for additional ω_0 values.

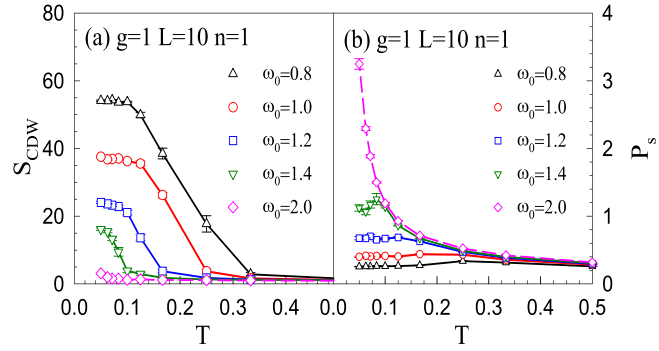

FIG. 1. DQMC results in the absence of dilution ($f = 0$). (a) CDW structure factor S_{cdw} on an $N = 10 \times 10$ lattice as a function of temperature T for $g = 1$ and half-filling, $\langle n\rangle = 1$. For smaller ω_0 there is a sharp increase in S_{cdw} for $T < T_{\text{cdw}}$, providing preliminary evidence of an ordered CDW phase. However, as ω_0 increases, charge correlations are diminished. (b) s-wave pairing susceptibility P_s as a function of T for the same parameters. P_s increases with increasing ω_0. For the largest phonon frequency, where S_{cdw} essentially vanishes, the pairing susceptibility grows dramatically at low T. For fixed $g/t = 1$, the phonon frequencies $\omega_0/t = 0.8, 1.0, 1.2, 1.4, 2.0$ correspond to dimensionless couplings $\lambda_D = g^2/(zt\omega_0) = 0.313, 0.250, 0.208, 0.179, 0.125$, respectively.

In order to discern CDW and SC phases, we define the equal-time, real-space charge correlation function,

$$c(\mathbf{r}) = \langle (\hat{n}_{\mathbf{i}\uparrow} + \hat{n}_{\mathbf{i}\downarrow})(\hat{n}_{\mathbf{i}+\mathbf{r}\uparrow} + \hat{n}_{\mathbf{i}+\mathbf{r}\downarrow})\rangle, \tag{3}$$

and its Fourier transform $S(\mathbf{q})$,

$$S(\mathbf{q}) = \sum_{\mathbf{r}} e^{i\mathbf{q}\cdot(\mathbf{r})} c(\mathbf{r}). \tag{4}$$

At commensurate filling $\langle n\rangle = 1$, the structure factor is sharply peaked at $\mathbf{q} = (\pi, \pi)$ owing to the perfect nesting of the noninteracting Fermi surface. Hence, we define $S_{\text{cdw}} \equiv S(\pi, \pi)$.

The s-wave pairing susceptibility is

$$P_s = \frac{1}{N}\int_0^{\beta} d\tau \langle \hat{\Delta}(\tau)\hat{\Delta}^{\dagger}(0)\rangle, \tag{5}$$

where $\hat{\Delta}(\tau) = \sum_{\mathbf{i}} \hat{c}_{\mathbf{i}\downarrow}(\tau)\hat{c}_{\mathbf{i}\uparrow}(\tau)$. We study SC via the (imaginary time integrated) susceptibility, rather than the equal time structure factor, because the former provides a more sensitive measure for pairing order, which is less robust than charge order.

$S(\mathbf{q})$ and P_s are both normalized in such a way that in a high-temperature or otherwise disordered phase, their values are independent of lattice size $N = L^2$ as long as $\xi \lesssim L$, where ξ is the correlation length. However, in an ordered phase with $\xi \gtrsim L$, S_{cdw} and P_s grow linearly with N. This provides an immediate, albeit somewhat crude, means by which long range order can be discerned.

Results. We start from the undiluted case, $f = 0$. In Fig. 1 we show S_{cdw} and P_s as functions of temperature T for electron-phonon coupling $g = t$ and varying phonon frequency ω_0, as well as linear lattice size $L = 10$ ($N = 100$).

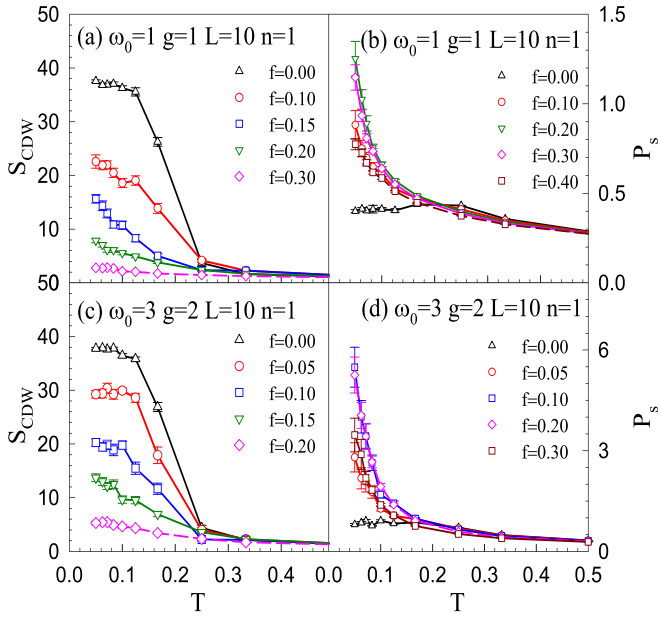

FIG. 2. CDW structure factor and s-wave pairing susceptibility as functions of T for different dilution fractions f. Starting from a CDW-dominant situation, f first enhances and then inhibits P_s, whereas it always inhibits $S_{\rm cdw}$.

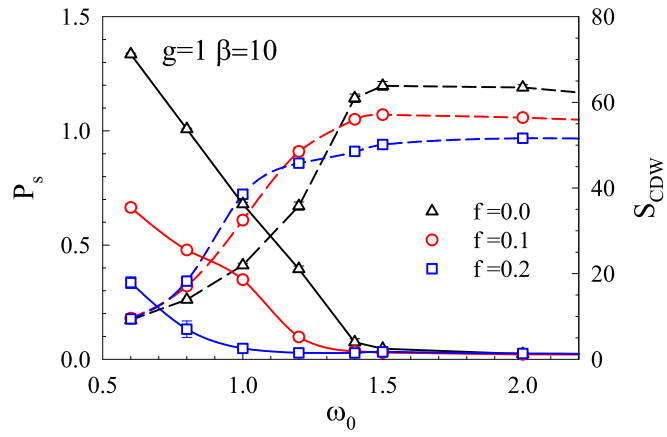

FIG. 3. Pairing and CDW correlations as functions of ω_0 for different dilution fractions. Dashed lines represent P_s while solid lines represent $S_{\rm cdw}$. The inverse temperature is fixed at $\beta t = 10$. CDW and SC compete, but coexistence is possible in the region of transition between them.

For $\omega_0 \lesssim 1.4t$ ($\lambda_D \gtrsim 0.18$), $S_{\rm cdw}$ rises sharply below a critical temperature that becomes smaller as the dimensionless coupling decreases (ω_0 increases). For small ω_0, there is no signal of superconductivity, since P_s is small and almost temperature independent. When the phonon frequency approaches $\omega_0 = 1.4t$, the pair structure factor grows as T decreases. This enhancement is, however, terminated at the temperature for which $S_{\rm cdw}$ rises, reflecting the competition of charge and pairing order. For the highest phonon frequency, $\omega_0 = 2t$, for which $S_{\rm cdw}$ remains small down to at least $T = t/20$, P_s shows an especially marked growth at low temperatures. That superconductivity is most easily observed in the antiadiabatic limit of large ω_0 is an established conclusion of prior QMC studies of the Holstein model [25,26].

Having briefly reviewed the charge and pair correlations in the clean limit to establish a baseline for comparison, we now explore nonzero dilution f. We begin, in Fig. 2, by choosing two parameter sets: $g = 1$, $\omega_0 = 1$ ($\lambda_D = 0.25$); and $g = 2$, $\omega_0 = 3$ ($\lambda_D = 0.33$). In both cases, λ_D is greater than the value $\lambda_D \sim 0.18$ above which the data of Fig. 1 show a sharp rise in $S_{\rm cdw}$ as T is lowered. Thus, charge correlations are dominant at $f = 0$ in these regimes, enabling us to investigate the effect of dilution on the small pairing correlations in a system that begins with a dominant CDW phase in the clean limit. Importantly, since the CDW gap completely gaps out the Fermi surface at half filling, the CDW phase is incompressible (i.e., insulating), characterized by a vanishingly small compressibility; we will return to this point later.

As shown in Fig. 2, dilution suppresses the CDW phase. For dilution $f = 0.1$, the value of $S_{\rm cdw}$ at $\beta t = 20$ is reduced by roughly a factor of two. In addition, the convergence of $S_{\rm cdw}$ to its ground state value is shifted to lower temperature. In contrast, the SC behavior is more complex. In the clean system, the pairing susceptibility P_s slowly decreases with decreasing temperature at low T. The introduction of dilution first significantly enhances the value of P_s and makes it grow sharply as $T \to 0$. This effect is strongest at $f \sim 0.1 - 0.2$. As f increases further, P_s decreases. Therefore, SC benefits from the destruction of CDW order with a small amount of dilution, but eventually too much dilution suppresses the electron-phonon coupling essential for pairing. While the two parameter sets show the same trends, the pairing correlations for larger $\omega_0 = 3$ [panel (d)] are significantly larger in magnitude than those for smaller $\omega_0 = 1$ [panel (b)].

This nonmonotonicity is reminiscent of the "superconducting dome" of the cuprates, and of the Hubbard model, where, in a similar way, doping first eliminates long range antiferromagnetic order, but too much doping removes the spin-fluctuations providing the pairing "glue." The analogy is incomplete, since in the Hubbard Hamiltonian there are only electronic degrees of freedom. Moreover, the role of remnant CDW fluctuations in mediating the pairing in the Holstein model is unclear [48,50].

An alternative display of the effects of dilution is shown in Fig. 3, where P_s and $S_{\rm cdw}$ at different f are shown as functions of ω_0. The most evident message, common to all values of f, is the competition between CDW and pairing order. The crossing between the two quantities is shifted to smaller ω_0 with increasing f. Moreover, for small ω_0, where CDW order is dominant, f enhances the pairing susceptibility, whereas in the absence of CDW order at large ω_0, dilution suppresses pairing.

The window of intermediate $\omega_0/t \sim 1$ in Fig. 3 raises the possibility of a coexistence of pairing and CDW orders induced by dilution. Such a phenomenon does not occur in the Holstein model with randomness introduced in the on-site energies [51]. In order to explore whether such a "supersolid" phase exists, we must perform a finite-size scaling study of the two order parameters.

We determine the window of supersolid regime in Fig. 4. We first ascertain the critical dilution that totally destroys

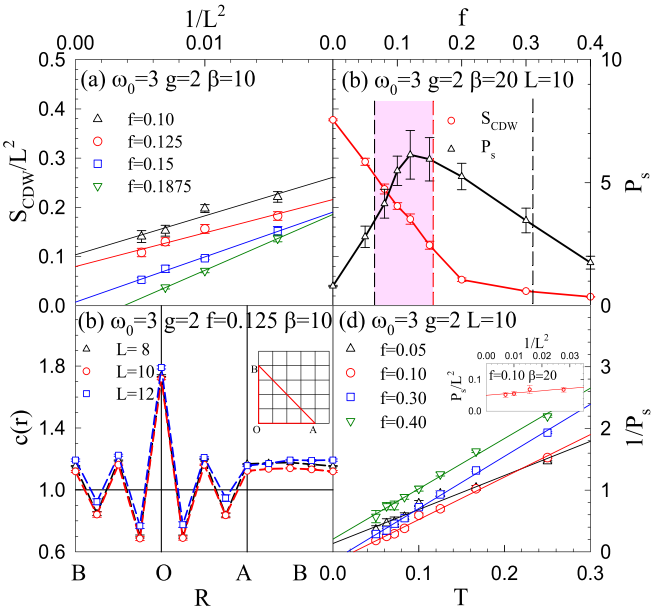

FIG. 4. (a) Normalized CDW correlations $S_{\rm cdw}/L^2$ as a function of inverse squared lattice size L^{-2}. A positive intercept represents long range order. (b) Pairing and normalized CDW correlations as functions of dilution fraction at a fixed low temperature ($\beta t = 20$). The red dashed line demarcates where CDW ends, and the black dashed lines give the range of SC order. Thus, the pink shaded region shows the supersolid phase. (c) Charge correlations $c(r)$ along the path shown in the inset. (d) $1/P_s$ as a function of T. For intermediate dilutions $f = 0.10$ and $f = 0.30$, $1/P_s$ vanishes at finite T. This divergence of the susceptibility signals a SC phase transition.

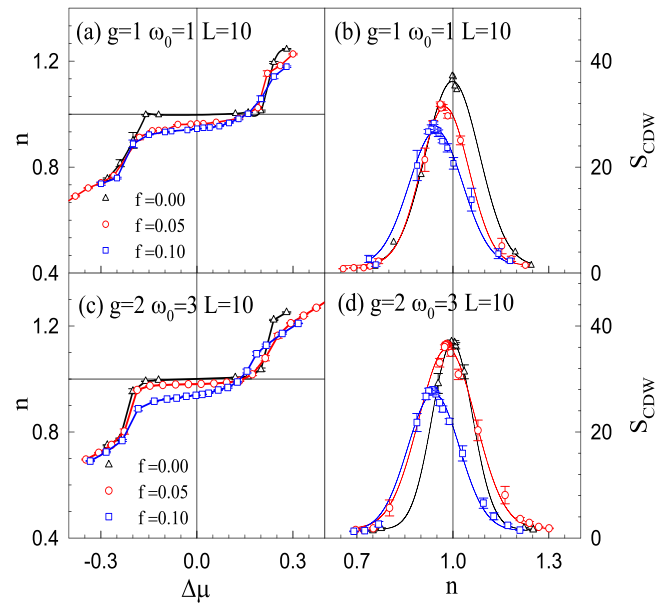

FIG. 5. Density $\langle n\rangle$ as a function of the shift in chemical potential $\Delta\mu$ away from $\mu_0 = -2g^2/\omega_0$, which gives half-filling in the clean ($f = 0$) limit. (a) $g = 1$, $\omega_0 = 1$ and (c) $g = 2$, $\omega_0 = 3$. $S_{\rm cdw}$ as a function of density n at (b) $g = 1$, $\omega_0 = 1$ and (d) $g = 2$, $\omega_0 = 3$. The peak of $S_{\rm cdw}$ is shifted from $\langle n\rangle = 1$ by f.

CDW order. In panel (a), we show the normalized CDW correlations as a function of $1/L^2$. When increasing f from $2/16$ to $3/16$, dilution suppresses $S_{\rm cdw}/L^2$ for each lattice size, and the intercept of the curve in the thermodynamic limit, which is the square of the CDW order parameter, goes to zero. Indeed, for $f \gtrsim 0.15$, $S_{\rm cdw}/L^2$ tends to zero when $L \to \infty$, suggesting that the CDW correlations are not long ranged and that there is short range order only. The real space charge correlation function $c(r)$ is shown in panel (c).

We now turn to the SC response. The reciprocal of the s-wave pairing susceptibility, $1/P_s$, is shown as a function of T in Fig. 4(d). For $f = 0.05$, P_s remains finite for all T, since $1/P_s$ does not vanish. However, for $f = 0.10$ and $f = 0.30$ there is a nonzero SC critical temperature, signaled by the fact that the extrapolated $1/P_s$ crosses the horizontal axis, that is, the P_s curve diverges at $T \to 0$. Increasing dilution further to $f = 0.40$ leads to the vanishing of long range SC order. We also show in the insert a finite value of normalized pairing susceptibility when extrapolated to $L \to \infty$ at $f = 0.10$, suggesting the dilution does enhance the SC long-rang order. We summarize the results in panel (b). While a SC phase exists in an intermediate dilution range, $f \in (0.075, 0.35)$, CDW order, which is dominant in the clean $f = 0$ limit, remains present up to $f \sim 0.15$. A supersolid window, where CDW and SC phases coexist, is present and centered around $f \sim 0.10$. The evolution of the single particle spectral function provides further evidence for the coexistence of CDW and SC order, as we show in the Supplemental Material [33].

The "conventional" picture of a SS phase is one of the condensation of mobile vacancies (e.g., through a shift of the chemical potential μ) whose motion does not sufficiently destroy the solid order. This scenario appears inapplicable here, since although we dilute the phonon degrees of freedom, we remain at half-filling for all the data of Fig. 4. Figures 5(a) and 5(c) lend insight into this question by showing the density $\langle n\rangle$ as a function of $\Delta\mu = \mu - \mu_0$, for different f values. Here, $\mu_0 = -2g^2/\omega_0$ is the chemical potential for half-filling of the clean system. What we observe is that, upon dilution, the plateau in $\langle n\rangle$ no longer occurs at commensurate filling $\langle n\rangle = 1$. In other words, the filling $n = 1$ is away from the filling which gives insulating behavior. In that sense, our system displays "self-doping." While the data shown are for a single realization, a discussion of disorder averaging is included in the Supplemental Material [33].

Figures 5(b) and 5(d) provide confirmation of this picture. $S_{\rm cdw}$ is shown as a function of filling $\langle n\rangle$ for different dilutions f. The most robust CDW order does not occur at $\langle n\rangle = 1$, but rather at a filling $\langle n\rangle \neq 1$ corresponding to the density at which the compressibility $\kappa = \partial\langle n\rangle/\partial\mu$ vanishes in panels (a) and (c). Thus, the filling $n = 1$ can be viewed as being doped away from the filling of largest CDW order. Further insight into this can be obtained by a calculation of the spectral function, shown in the Supplemental Material [33].

Discussion. The experimental search for supersolidity in Helium [5], although later rebutted [7], had nevertheless an intriguing premise: by placing the Helium in the porous environment of Vycor glass, the number of delocalized vacancies associated with zero point fluctuations of the quantum solid might be enhanced, thereby increasing the tendency to superfluidity.

Inspired by this general idea, in this work, using DQMC simulations, we have studied the effect of a fractional dilution f of local oscillators in the Holstein Hamiltonian on the competition between superconductivity and charge density wave formation. Through an analysis of the CDW structure factor and SC susceptibility we provide evidence that a SS phase can be induced even at half filling. The seemingly surprising occurrence of a SS without (carrier) dilution is explained by the fact that that even though the fermion filling $\langle n \rangle$ nominally remains at the commensurate value $\langle n \rangle = 1$ (no "vacancies"), the shift in the optimal filling for CDW order away from half-filling effectively results in vacancies at $\langle n \rangle = 1$.

One of the obstacles to conventional supersolid formation is the possibility of phase separation of the mobile vacancies, a phenomenon known to obscure supersolid formation for bosonic systems on square lattices [52]. The realization of supersolidity presented here avoids that obstacle, because the phonon dilution pattern is fixed in space. Thus, the mobile vacancies that are introduced are necessarily spread out spatially.

It is interesting to ask whether the dilute Holstein model studied here could be realized in materials. While an in-depth analysis is beyond the scope of this work, we note that transition metal dichalcogenides (TMDs) are well known for displaying CDW which, in some cases, coexists with or is in proximity to a SC phase. More specifically, this is the case of two nonmetallic TMDs: $1T$-$TiSe_2$, which displays semiconductinglike transport properties in the CDW state [53,54], and $1T$-TaS_2, which is believed to be a Mott insulator in the CDW phase [55,56]. In the case of $1T$-$TiSe_2$, Cu intercalation [53] or pressure [54] suppresses the CDW phase and promotes SC, with both states overlapping in the phase diagram. Because Cu is introduced between the Ti-Se layers, it is expected to locally affect the crystal structure, which in turn should cause a local change in the electron-phonon interaction, as the atoms will be displaced from their original positions. In the case of $1T$-TaS_2, it has been shown that application of pressure [55] leads to a SC phase as the CDW is suppressed, with a possible region of coexistence. However, whether SC occurs in Cu intercalated samples remains to be seen [56]. Recently, it has been confirmed that Pd intercalation induces disorder in the crystal lattice of ErTe3, suppressing CDW formation and leading to a SC ground state [57].

Of course, the microscopic description of these two materials is much more complicated than our simple model—for instance, Cu intercalation also adds charge carriers in the case of $1T$-$TiSe_2$. Nevertheless, it is an interesting possibility that intercalation in nonmetallic CDW TMDs can provide a mechanism for a spatially inhomogeneous electron-phonon coupling.

Acknowledgments. J.M. and T.M. were supported by the NSFC (12474218) and the Beijing Natural Science Foundation (No. 1242022), and the work of R.S. was supported by Grant DE-SC0014671 funded by the U.S. Department of Energy, Office of Science. Y.Z. and R.M.F. were supported by the Air Force Office of Scientific Research under Award No. FA9550-21-1-0423.

[1] O. Penrose and L. Onsager, Bose-Einstein condensation and liquid helium, Phys. Rev. **104**, 576 (1956).
[2] A. Andreev and I. Lifshits, Quantum theory of defects in crystals, Zhur Eksper Teoret Fiziki **56**, 2057 (1969).
[3] G. Chester, Speculations on Bose-Einstein condensation and quantum crystals, Phys. Rev. A **2**, 256 (1970).
[4] A. J. Leggett, Can a solid be "superfluid"? Phys. Rev. Lett. **25**, 1543 (1970).
[5] E. Kim and M. H.-W. Chan, Probable observation of a supersolid helium phase, Nature (London) **427**, 225 (2004).
[6] X. Mi and J. D. Reppy, Anomalous behavior of solid ^{4}He in porous Vycor glass, Phys. Rev. Lett. **108**, 225305 (2012).
[7] D. Y. Kim and M. H. W. Chan, Absence of supersolidity in solid helium in porous Vycor glass, Phys. Rev. Lett. **109**, 155301 (2012).
[8] R. T. Scalettar, G. G. Batrouni, A. P. Kampf, and G. T. Zimanyi, Simultaneous diagonal and off-diagonal order in the Bose-Hubbard Hamiltonian, Phys. Rev. B **51**, 8467 (1995).
[9] A. Van Otterlo, K.-H. Wagenblast, R. Baltin, C. Bruder, R. Fazio, and G. Schön, Quantum phase transitions of interacting bosons and the supersolid phase, Phys. Rev. B **52**, 16176 (1995).
[10] E. Frey and L. Balents, Critical behavior of the supersolid transition in Bose-Hubbard models, Phys. Rev. B **55**, 1050 (1997).
[11] S. Wessel and M. Troyer, Supersolid hard-core bosons on the triangular lattice, Phys. Rev. Lett. **95**, 127205 (2005).
[12] R. G. Melko, A. Paramekanti, A. A. Burkov, A. Vishwanath, D. N. Sheng, and L. Balents, Supersolid order from disorder: Hard-core bosons on the triangular lattice, Phys. Rev. Lett. **95**, 127207 (2005).
[13] N. Laflorencie and F. Mila, Quantum and thermal transitions out of the supersolid phase of a 2D quantum antiferromagnet, Phys. Rev. Lett. **99**, 027202 (2007).
[14] J. Xiang, C. Zhang, Y. Gao, W. Schmidt, K. Schmalzl, C.-W. Wang, B. Li, N. Xi, X.-Y. Liu, H. Jin *et al.*, Giant magnetocaloric effect in spin supersolid candidate $Na_2BaCo(PO_4)_2$, Nature (London) **625**, 270 (2024).
[15] T. Chen, A. Ghasemi, J. Zhang, L. Shi, Z. Tagay, L. Chen, E.-S. Choi, M. Jaime, M. Lee, Y. Hao *et al.*, Phase diagram and spectroscopic evidence of supersolids in quantum Ising magnet $K_2Co(SeO_3)_2$, arXiv:2402.15869.
[16] J.-R. Li, J. Lee, W. Huang, S. Burchesky, B. Shteynas, F. Ç. Top, A. O. Jamison, and W. Ketterle, A stripe phase with supersolid properties in spin–orbit-coupled Bose–Einstein condensates, Nature (London) **543**, 91 (2017).
[17] J. Léonard, A. Morales, P. Zupancic, T. Esslinger, and T. Donner, Supersolid formation in a quantum gas breaking a continuous translational symmetry, Nature (London) **543**, 87 (2017).
[18] L. Tanzi, S. Roccuzzo, E. Lucioni, F. Famà, A. Fioretti, C. Gabbanini, G. Modugno, A. Recati, and S. Stringari, Supersolid symmetry breaking from compressional oscillations in a dipolar quantum gas, Nature (London) **574**, 382 (2019).
[19] M. A. Norcia, C. Politi, L. Klaus, E. Poli, M. Sohmen, M. J. Mark, R. N. Bisset, L. Santos, and F. Ferlaino, Two-dimensional

supersolidity in a dipolar quantum gas, Nature (London) **596**, 357 (2021).
[20] T. Holstein, Studies of polaron motion: Part I. The molecular-crystal model, Ann. Phys. **8**, 325 (1959).
[21] M. Hohenadler, Interplay of site and bond electron-phonon coupling in one dimension, Phys. Rev. Lett. **117**, 206404 (2016).
[22] Y.-X. Zhang, W.-T. Chiu, N. C. Costa, G. G. Batrouni, and R. T. Scalettar, Charge order in the Holstein model on a honeycomb lattice, Phys. Rev. Lett. **122**, 077602 (2019).
[23] B. Xing, W.-T. Chiu, D. Poletti, R. T. Scalettar, and G. Batrouni, Quantum Monte Carlo simulations of the 2D Su-Schrieffer-Heeger model, Phys. Rev. Lett. **126**, 017601 (2021).
[24] N. C. Costa, W. Hu, Z. J. Bai, R. T. Scalettar, and R. R. P. Singh, Principal component analysis for fermionic critical points, Phys. Rev. B **96**, 195138 (2017).
[25] O. Bradley, G. G. Batrouni, and R. T. Scalettar, Superconductivity and charge density wave order in the two-dimensional Holstein model, Phys. Rev. B **103**, 235104 (2021).
[26] B. Nosarzewski, E. W. Huang, P. M. Dee, I. Esterlis, B. Moritz, S. A. Kivelson, S. Johnston, and T. P. Devereaux, Superconductivity, charge density waves, and bipolarons in the Holstein model, Phys. Rev. B **103**, 235156 (2021).
[27] A. T. Ly, B. Cohen-Stead, S. M. Costa, and S. Johnston, Comparative study of the superconductivity in the Holstein and optical Su-Schrieffer-Heeger models, Phys. Rev. B **108**, 195415 (2023).
[28] M. V. Araújo, J. P. de Lima, S. Sorella, and N. C. Costa, Two-dimensional $t - t'$ Holstein model, Phys. Rev. B **105**, 165103 (2022).
[29] M. Vekić, R. M. Noack, and S. R. White, Charge-density waves versus superconductivity in the Holstein model with next-nearest-neighbor hopping, Phys. Rev. B **46**, 271 (1992).
[30] M. Weber and M. Hohenadler, Two-dimensional Holstein-Hubbard model: Critical temperature, Ising universality, and bipolaron liquid, Phys. Rev. B **98**, 085405 (2018).
[31] N. C. Costa, T. Blommel, W.-T. Chiu, G. Batrouni, and R. T. Scalettar, Phonon dispersion and the competition between pairing and charge order, Phys. Rev. Lett. **120**, 187003 (2018).
[32] S. Sykora, A. Huebsch, and K. W. Becker, Coexistence of superconductivity and charge-density waves in a two-dimensional Holstein model at half-filling, Europhys. Lett. **85**, 57003 (2009).
[33] See Supplemental Material at http://link.aps.org/supplemental/10.1103/PhysRevB.110.L220506 for the further discussion of disorder averaging, the spectral function and compressibility, which also contains Refs. [34–46].
[34] P.-E. Berche, C. Chatelain, B. Berche, and W. Janke, Bond dilution in the 3D Ising model: a Monte Carlo study, Eur. Phys. J. B **38**, 463 (2004).
[35] H. G. Ballesteros, L. A. Fernández, V. Martín-Mayor, A. Muñoz Sudupe, G. Parisi, and J. J. Ruiz-Lorenzo, Critical exponents of the three-dimensional diluted ising model, Phys. Rev. B **58**, 2740 (1998).
[36] S. Wiseman and E. Domany, Self-averaging, distribution of pseudocritical temperatures, and finite size scaling in critical disordered systems, Phys. Rev. E **58**, 2938 (1998).
[37] A. Aharony, A. B. Harris, and S. Wiseman, Critical disordered systems with constraints and the inequality $\nu > 2/D$, Phys. Rev. Lett. **81**, 252 (1998).
[38] K. Machida, Charge density wave and superconductivity in anisotropic materials, J. Phys. Soc. Jpn. **53**, 712 (1984).
[39] R. M. Fernandes and J. Schmalian, Competing order and nature of the pairing state in the iron pnictides, Phys. Rev. B **82**, 014521 (2010).
[40] J. Kaufmann and K. Held, ana_cont: Python package for analytic continuation, Comput. Phys. Commun. **282**, 108519 (2023).
[41] J. Fei, C.-N. Yeh, and E. Gull, Nevanlinna analytical continuation, Phys. Rev. Lett. **126**, 056402 (2021).
[42] K. Ghanem and E. Koch, Average spectrum method for analytic continuation: Efficient blocked-mode sampling and dependence on the discretization grid, Phys. Rev. B **101**, 085111 (2020).
[43] L. Huang, ACFlow: An open source toolkit for analytic continuation of quantum Monte Carlo data, Comput. Phys. Commun. **292**, 108863 (2023).
[44] J. S. Hofmann, E. Berg, and D. Chowdhury, Superconductivity, charge density wave, and supersolidity in flat bands with a tunable quantum metric, Phys. Rev. Lett. **130**, 226001 (2023).
[45] M. Iskin and C. A. R. Sá de Melo, Nonzero orbital angular momentum superfluidity in ultracold Fermi gases, Phys. Rev. A **74**, 013608 (2006).
[46] K.-W. Lee, J. Kuneš, R. T. Scalettar, and W. E. Pickett, Correlation effects in the triangular lattice single-band system Li_xNbO_2, Phys. Rev. B **76**, 144513 (2007).
[47] R. Blankenbecler, D. J. Scalapino, and R. L. Sugar, Monte Carlo calculations of coupled boson-fermion systems. I, Phys. Rev. D **24**, 2278 (1981).
[48] R. T. Scalettar, N. E. Bickers, and D. J. Scalapino, Competition of pairing and Peierls–charge-density-wave correlations in a two-dimensional electron-phonon model, Phys. Rev. B **40**, 197 (1989).
[49] M. Creutz and B. A. Freedman, A statistical approach to quantum mechanics, Ann. Phys. **132**, 427 (1981).
[50] N. Bickers, D. Scalapino, and R. Scalettar, CDW and SDW mediated pairing interactions, Int. J. Mod. Phys. B **1**, 687 (1987).
[51] B. Xiao, N. C. Costa, E. Khatami, G. G. Batrouni, and R. T. Scalettar, Charge density wave and superconductivity in the disordered Holstein model, Phys. Rev. B **103**, L060501 (2021).
[52] G. G. Batrouni and R. T. Scalettar, Phase separation in supersolids, Phys. Rev. Lett. **84**, 1599 (2000).
[53] E. Morosan, H. W. Zandbergen, B. Dennis, J. Bos, Y. Onose, T. Klimczuk, A. Ramirez, N. Ong, and R. J. Cava, Superconductivity in Cu_xTiSe_2, Nat. Phys. **2**, 544 (2006).
[54] A. F. Kusmartseva, B. Sipos, H. Berger, L. Forró, and E. Tutiš, Pressure induced superconductivity in pristine 1t-$TiSe_2$, Phys. Rev. Lett. **103**, 236401 (2009).
[55] B. Sipos, A. F. Kusmartseva, A. Akrap, H. Berger, L. Forró, and E. Tutiš, From Mott state to superconductivity in 1T-TaS_2, Nat. Mater. **7**, 960 (2008).
[56] E. Lahoud, O. N. Meetei, K. B. Chaska, A. Kanigel, and N. Trivedi, Emergence of a novel pseudogap metallic state in a disordered 2D Mott insulator, Phys. Rev. Lett. **112**, 206402 (2014).
[57] Y. Iguchi, J. A. Straquadine, C. Murthy, S. A. Kivelson, A. G. Singh, I. R. Fisher, and K. A. Moler, Anomalous superfluid density in a disordered charge-density-wave material: Pd-intercalated $ErTe_3$, Phys. Rev. Lett. **133**, 036001 (2024).